Bulletin of Faculty of Science, Zagazig University (BFSZU)
e-ISSN: 1110-1555
Volume-2025, Issue-1, pp-141-152
https://bfszu.journals.ekb.eg/journal
Research Paper DOI: **10.21608/bfszu.2024.299799.1403**

Design, synthesis, and computational studies as cytotoxicity of novel pyrimidine carbonitrile derivatives as dual-target inhibitors of BRD4.

Hend A. Haikal [1], Wesam S. Shehab [1], Ahmed F. EL-Farargy [1], Abdel Rahman B.A.El-Gazzar [3], Doaa A. Elsayed [1]*

1Department of Chemistry, Faculty of Science, Zagazig University, Zagazig 44519, Egypt;

1 Correspondence: doaaatef641995@gmail.com, doaaatef@zu.edu.eg).*

ABASTRACT : ***Structural-based drug design was employed to create new pyrimidine carbonitrile compounds for dual BRD4. The compounds were identified using IR, ^{1}H-NMR, ^{13}C-NMR, and mass spectra. The compounds fit the volasertib binding site at BRD4 and exhibit drug-like characteristics and pharmacokinetics, making them potential anticancer candidates. All of the compounds interacted with the highest number of targets. Compound 1 had the greatest interactions, engaging with four anticancer targets (5V67, 3FC2, 3IG7, and 4ASD). Compare the ADME study results for compounds 1–3 to those for volasertib. Overall, all of the rule principles that might indicate drug-likeness for the tested compounds 1, 2, and 3 performed admirably, suggesting that these substances may fulfill the cell membrane permeability and bioavailability criteria. All 3 targets associated with anti-cancer illness were docked separately with each medication. These compounds have extraordinarily high binding affinities for all 3 anticancer targets. Compounds 1, 2, and 3 showed similar interactions to Volasertib when docked into BRD4 active sites. These compounds also demonstrated superior drug-likeness and pharmacokinetics compared to Volasertib itself.***
KEYWORDS BRD4 ; pyrimidine carbonitrile; cytotoxicity; Molecular docking.

Date of Submission: 04-07-2024 Date of acceptance: 20-10-2024

I. RATIONALE STRATEGY FOR DESIGNING THE NEW TARGETS

Volasertib was shown to attach to the BRD4 binding site, creating a hydrogen bond with the crucial amino acid. The amino pyrimidine moiety was responsible for the remaining hydrophobic interactions **(El-Kalyoubi, El-Sebaey, Elfeky, Al-Ghulikah, & El-Zoghbi, 2023; Karim et al., 2021)**. To achieve the previously described binding interactions, structure-based design and structural changes of known active cores were employed to generate a series of pyrimidine carbonitrile derivatives as dual BRD4 inhibitors. Computational (in silico) investigations (molecular docking simulation, drug-likeness, and ADME profile studies) were conducted to investigate the mechanism of binding to BRD4's active site in order to determine their potential as anticancer candidates **Figure (1)**.

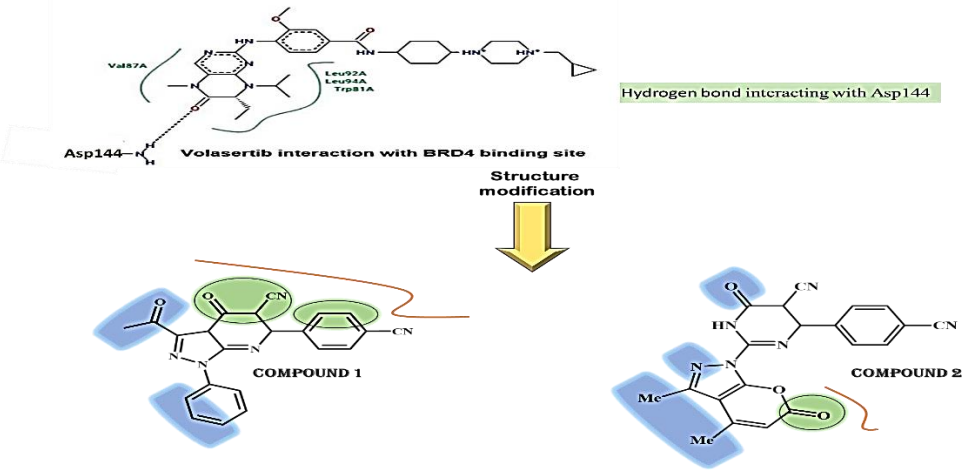

Figure 1. Design rationale and work goal

II. INTRODICUCTION

As one of the top two causes of death before the age of 70 in many nations, cancer is a severe public health concern with implications worldwide **(Bray et al., 2018; Elkady et al., 2023)**.

Surgery has long been one of the primary therapeutic approaches for cancer treatment. It is often the first option for localized tumors, as it aims to remove as much cancerous tissue as possible, potentially leading to a cure if the cancer hasn't spread. However, the effectiveness and feasibility of surgery depend on several factors: Location of the cancer: Tumors located in sensitive or hard-to-reach areas, such as near vital organs or deep inside the body, may make surgery risky or less effective. Severity and Stage: Early-stage cancers are often more amenable to surgery, while advanced or metastatic cancers (those that have spread to other parts of the body) are typically not suitable for surgical intervention. Patient's Overall Health: Surgery is invasive and may not be an option for patients with compromised health or those who might not tolerate anesthesia and the recovery process.

Non-Surgical Treatment Options: When surgery isn't possible or suitable, a variety of non-surgical treatments can be employed, often in combination, to target cancer in different ways: Radiation Therapy: Uses high-energy radiation to kill cancer cells or shrink tumors. It is often used for localized cancers or as an adjunct to surgery to remove any remaining cancer cells. Chemotherapy: Involves the use of drugs to destroy rapidly growing cancer cells. It is used for cancers that have spread or cannot be surgically removed, often combined with other treatments. Immunotherapy: Aims to stimulate the body's immune system to recognize and attack cancer cells. This is particularly effective in certain cancers, like melanoma, and can be used when surgery isn't viable. Targeted Therapy: These treatments target specific molecules involved in cancer growth, sparing normal cells and causing fewer side effects compared to traditional chemotherapy.

These non-surgical methods can be effective, especially for cancers that have spread or are difficult to access surgically, and may also be used in combination with surgery to improve outcomes. Each treatment option has its own benefits and risks, and the choice often depends on the specific type of cancer, its progression, and the patient's overall health **(Mabrouk et al., 2023; Penna, Henriques, & Bonatto, 2017)**. The intricacy of the disease stemming from the unchecked proliferation and division of aberrant cells within the body, which is initiated by malfunctioning regulation of various signaling pathways, means that despite all of these choices, treating cancer remains a major challenge for doctors and researchers. These include the overexpression of anti-apoptotic proteins like Bcl-2 and the deregulation of many kinases **(Saleh et al., 2023; Zhang, Yang, & Gray, 2009)**. Current cancer treatments have been associated with drug resistance and recurrence in certain cases, prompting the creation of novel therapeutic approaches such combination drugs that target multiple signaling pathways **(Mokhtari et al., 2017)**.

By specifically targeting numerous pathways, dual inhibitors represent a significant area in the seek for novel cancer therapeutics that have the potential to overcome drug resistance and enhance therapeutic results for cancer patients **(Watts et al., 2019)**. In comparison to single-drug therapy, a number of medication combinations that include kinase inhibitors and epigenetic regulatory agents have been shown to be more effective in preclinical cancer models and clinical trials **(Mao et al., 2018)**. The protein known as bromodomain-containing protein 4 (BRD4) is a member of the BET protein family and possesses an epigenetic reader domain. These proteins bind to acetylated lysine residues on histones and recruit transcriptional machinery, which is crucial for controlling gene expression for cell survival (e.g., Bcl-2) and proliferation (e.g., c-Myc, Aurora B)**(Dong et al., 2022; Wyce et al., 2013)**. Numerous physiological processes, such as the progress of the cell cycle, the DNA damage response, and inflammation—which has been linked to the onset of multiple diseases, including cancer and inflammatory disorders—depend on BRD4 **(Lambert et al., 2019)**.

Numerous cancer types, including hematological malignancies, prostate, lung, and breast cancers, have been shown to overexpress BRD4 **(Vann et al., 2020)**. Recent studies have demonstrated that BRD4 is involved in various cellular processes that contribute to the spread of cancer, in addition to controlling gene expression. One example is how BRD4 interacts with crucial proteins involved in DNA repair to regulate DNA damage response pathways **(Yuzwa et al., 2017)**. Therefore, finding possible new BRD4 dual-target inhibitors may be a useful strategy for treating cancer.

In both preclinical research and clinical trials, structurally varied cores of BRD4 inhibitors have demonstrated strong anticancer effectiveness against a range of cancer types. These cores include imidazoquinoline (I-BET151 or GSK1210151A) (III) **(Seal et al., 2012)**, pyrrolopyridine (ABBV-744 in phase I) (II) **(Faivre et al., 2020)**, and quinazoline (Apabetalone or RVX-208 in phase II) (1) **(Picaud et al., 2013)**.

We also studied the manufactured drugs using molecular docking, which can predict the most frequent binding mode(s) of a receptor with a protein in a three-dimensional geometry **(Aziz, Shehab, Al-Karmalawy, EL-Farargy, & Abdellattif, 2021; Kukol, 2008; Morris & Lim-Wilby, 2008)**. This study synthesized many pyrimidine carbonitrile derivatives by novel methods. The compounds were identified using IR, ^{1}H-NMR, ^{13}C-NMR, and mass spectra. The experimental data were obtained by computational investigations (molecular docking) using MOE (2022).

II. EXPERIMENTAL

Materials and methods

High-quality materials were used to perform this research. Sigma-Aldrich supplied all of the chemicals (triethylamine 99.5%, 2-oxo-N-phenylpropanehydrazonoyl chloride 97%, ethyl acetoacetate 99%, p-nitrobenzaldehyde 98.5%) (Taufkirchen, Germany). El-Nasr Pharmaceutical Chemicals Company provided all solvents (ethanol 99.8%, chloroform 99.8%) (analytical reagent grade, Egypt). The melting points were measured using a Cole-Parmer digital Electrothermal IA 9100 Series (Beacon Road, Stone, Staffordshire, ST15 OSA, UK) and are uncorrected. C, H, and N analyses were performed using a PerkinElmer CHN 2400. The FT-IR 460 PLUS was used to generate IR spectra (KBr disks). A Bruker 400, 100 MHz NMR Spectrometer was used to generate ^{1}H and ^{13}C-NMR spectra, with DMSO-d_6 as the solvent and chemical shifts expressed in (ppm) at the Main Laboratories of Chemical War, Nasr City, Egypt. Thin-layer chromatography (TLC) sheets covered with UV fluorescent silica gel Merck 60 F254 plates were used to monitor the reactions, which were monitored with a UV laser and different solvents as mobile phases. MOE software (2022) was used to conduct molecular docking investigations.

synthesis

3-acetyl-6-(4-cyanophenyl)-4-oxo-1-phenyl-3a,4,5,6-tetrahydro-1H-pyrazolo[3,4-b]pyridine-5-carbonitrile (1)

Reflux was performed for seven hours on the compound 4-(4-cyanophenyl)-6-oxo-2-thioxohexahydropyrimidine-5-carbonitrile (0.0005 mol), 1 mL triethylamine, 0.22 g, 0.0011 mol, and 2-oxo-N-phenylpropanehydrazonoyl chloride in (30 mL) chloroform. Following cooling, the resultant solid **1** was filtered and then crystallized from 50 milliliters of ethanol; the yield was 42% and the melting point was 205-207 °C (decomposed). IR (KBr, ν, cm-1): 3013- 2891 cm-1 (CH for aromatic and aliphatic), 2242 cm-1 (CN), 1644 cm^{-1}(2 C=O). ^{1}H-NMR (DMSO-d_6, 500 MHz): δ = 3.34 (d, 1H, methine-CH-CN), 2.49 (d,1H, CH(CN)- CH-Ar), 1.78 (s, 3H, CH_3-C=O), 7.4,8.06 (d, d, 4H, CH Aromatic). ^{13}C-NMR (DMSO-d_6, 125 MHz): δ = 24.51, 25.34, 39.50, 45.56, 80.88, 85.78, 109.8, 121.70, 122.97, 128.76, 128.86, 128.98, 129.32, 129.54, 129.69, 132.72, 147.31,140.4, 154.96, 168.09 ppm. Anal. Calcd. for $C_{21}H_{14}N_6O_2$ (382.38): C, 65.96; H, 3.69; N, 21.98.

4-(4-cyanophenyl)-2-(3,4-dimethyl-6-oxopyrano[2,3-c]pyrazol-1(6H)-yl)-6-oxo-1,4,5,6-tetrahydropyrimidine-5-carbonitrile (2)

Compound 4-(4-cyanophenyl)-2-hydrazineyl-6-oxo-1,4,5,6-tetrahydropyrimidine-5-carbonitrile (10 mmol) and 30 mL of excess ethyl acetoacetate were heated to reflux temperature for six hours. Following the addition of the combination to ice-cold water, the resulting product was dried, rinsed with water, and then recrystallized from ethanol to provide a pale brown powder of the pyrazolone compound **2** (yield: 51%; mp: 230–232°C). IR (KBr, ν, cm^{-1}): 3250 cm^{-1} (NH str), 3075- 2983cm^{-1} (CH for aromatic and aliphatic), 2224 cm^{-1} (CN), 1735, 1687 cm^{-1}(C=O). ^{1}H-NMR (DMSO-d_6, 500 MHz): δ = 3.57 (d, 1H, methine-CH-CN), 2.49 (d,1H, CH(CN)-CH-Ar), 7.07,7.9 (d, d, 4H, CH Aromatic), 5.8 (s,1H, pyranone ring) 8.05 ppm (NH exchangeable with D_2O), 2.46, 2.34(s,2CH_3). Anal. Calcd. for $C_{20}H_{14}N_6O_3$(386.37): C, 62.17; H, 3.65; N, 21.75

(E)-4-(4-cyanophenyl)-2-(2-(4-nitrobenzylidene)hydrazineyl)-6-oxo-1,4,5,6-tetrahydropyrimidine-5-carbonitrile (3)

Compound 4-(4-cyanophenyl)-2-hydrazineyl-6-oxo-1,4,5,6-tetrahydropyrimidine-5-carbonitrile (10 mmol) was mixed with 10 mmol of p-nitrobenzaldehyde and 45 mL of 100% ethanol. After being refluxed for six hours and concentrated to half its original volume, the liquid was left to cool. Compound **3** (yield 75%; mp 250–252

°C) was obtained by recrystallizing the resultant precipitate from ethanol. IR (KBr, ν, cm^{-1}): 3250 cm^{-1} (NH str), 3100- 2820cm^{-1} (CH for aromatic and aliphatic), 2226 cm^{-1} (CN), 1675 cm^{-1}(C=O), 1511, 1413 (NO_2), 1568 cm^{-1} (C=N). ^{1}H-NMR (DMSO-d_6, 500 MHz): δ = 3.34 (d, 1H, methine-CH-CN), 2.49 (d,1H, CH(CN)-CH-Ar), 8.14, 8.21(d, d, 4H, CH Aromatic), 7.94, 7.98 (d, d, 4H, CH Aromatic), 10.8 ppm (2NH exchangeable with D_2O), 8.4 (s, 1H, azomethine-HN =CH)). Anal. Calcd. for $C_{19}H_{13}N_7O_3$(387.36): C, 58.91; H, 3.38; N, 25.31

Molecular Docking Simulation

Molecular docking simulation was performed using the Molecular Operating Environment (MOE) software 2022, as described in the literature **(Elfeky, Almehmadi, & Tawfik, 2022; Hamed, Assy, Ouf, Elsayed, & Abdellattif, 2022; Shehab et al., 2024)**. The MOE builder was used to create ligands, which were then 3D protonated and assigned partial charges before being energy-minimized with the MMFF94x force field. Volasertib was used to target the binding sites of BRD4 (PDB ID:5V67) (Karim et al., 2021), PLK1 (PDB ID: 3FC2) **(Rudolph et al., 2009)**, (PDB ID: 3IG7) **(Umar et al., 2022)**, and (PDB ID: 4ASD) **(Kumar et al., 2022)**, which were retrieved from the RCSB-Protein Data Bank. Proteins were created utilizing conventional protocols, including 3D-protonation and automated correction for atom types and linkages. They were then possibly repaired. MOE's alpha site finder was used to determine active sites. MOE's induced fit docking methodology was employed. The usual validation methodology involved re-docking the native ligand against the active sites of 5V67, with RMSD values <2.0 Å. The triangle matcher technique and London dG scoring function were used to study ligand interactions at active sites using bond rotation as a first scoring function. The GBVI/WSA dG forcefield-based scoring mechanism was used as a second scoring function, resulting in five poses out of thirty. Poses with greater S-values and lower RMSD were recorded **(Hamed, Elsayed, Assy, & Shehab, 2022)**.

The Predicted Drug-Likeness and ADME Properties

In silico bioinformatic studies were conducted on promising compounds **1**, **2**, and **3** to predict their physicochemical properties (size, lipophilicity, solubility, polarity, and flexibility), as well as pharmacokinetics (GIT absorption, distribution, and metabolism by the liver metabolizing enzyme Cytochrome P450). Additionally, if they are orally bioavailable candidates (based on Lipinski's rule) compared to volasertib. The compounds' drug-likeness and ADME characteristics were analyzed using the Swiss ADME online program **(www.SwissADME.ch/, accessed on May 2, 2023) (Daina, Michielin, & Zoete, 2017; Shehab, Amer, Elsayed, Yadav, & Abdellattif, 2023)**.

III. Results and Discussion

Chemistry

On the basis of the pyrimidine moiety, several novel heterocyclic compounds were developed. Compound 4-(4-cyanophenyl)-6-oxo-2-thioxohexahydropyrimidine-5-carbonitrile produced 3-acetyl-6-(4-cyanophenyl)-4-oxo-1-phenyl-3a,4,5,6-tetrahydro-1H-pyrazolo[3,4-b]pyridine-5-carbonitrile **1** when it interacted with 2-oxo-N-phenylpropanehydrazonoyl chloride in chloroform with few drops of triethylamine **Scheme (1)**.

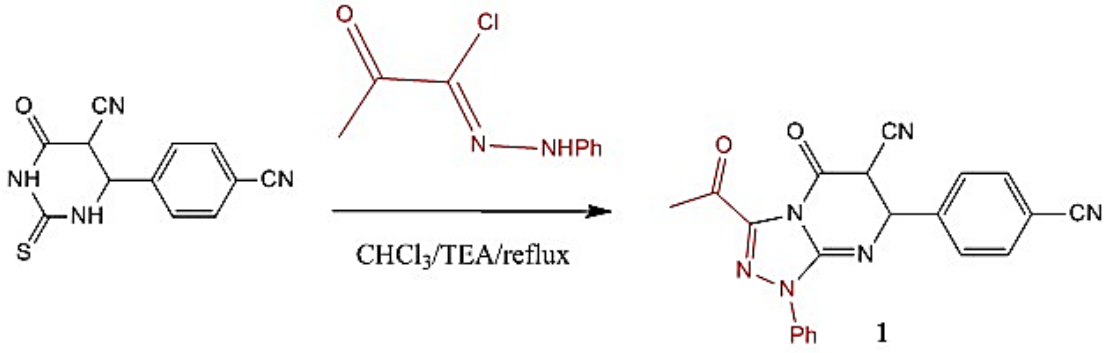

Scheme 1 : Synthesis of substituted pyrazolopyrimidine carbonitrile

The most plausible pathway for the development of compound **1** through the reaction between 4-(4-cyanophenyl)-6-oxo-2-thioxohexahydropyrimidine-5-carbonitrile and 2-oxo-N-phenylpropanehydrazonoyl chloride is represented by the mechanism of synthesis compound 1, as shown in **Scheme (2)**. This is based on the previously described findings. Thiohydrazonates (A) are first synthesized, and then intermolecular cyclization occurs shortly after to yield the Spiro intermediate (B). The final product 1 are obtained from ring chain tautomerism of Spiro intermediate C by removing hydrogen sulfide.

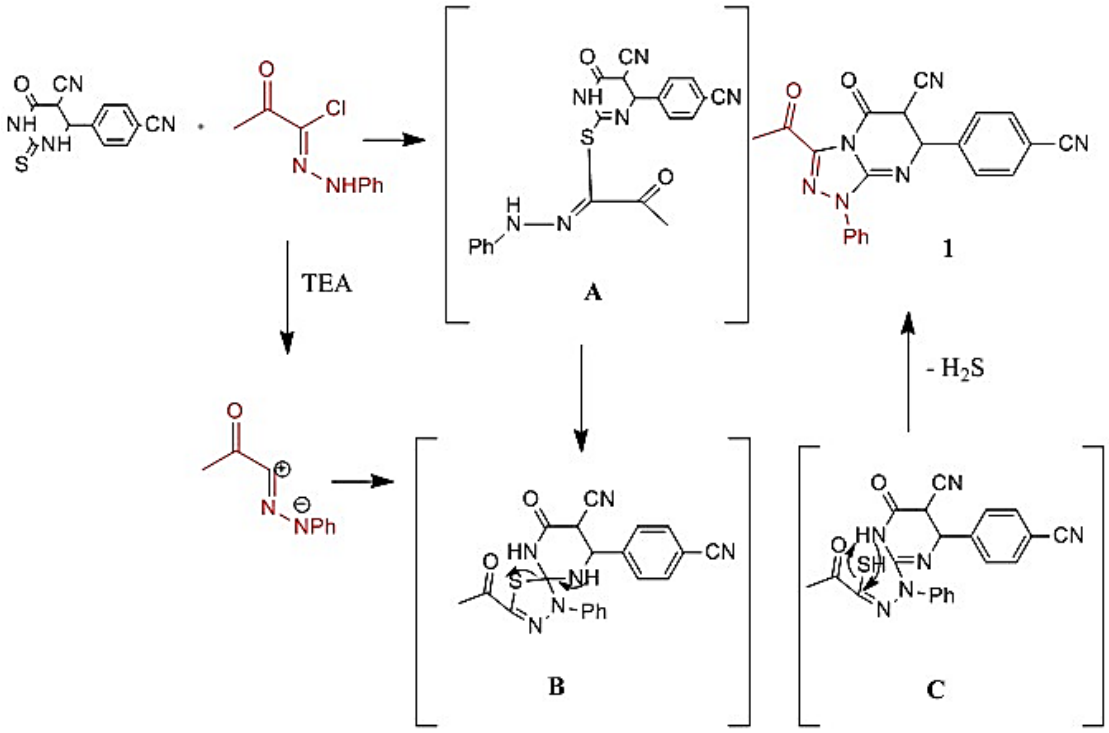

Scheme 2: The possible mechanism for the synthesis of Tetrahydro-4-oxo-1-phenyl-3a,4,5,6-1H-pyrazolo[3,4-b]5-carbonitrile pyridine (1)

Because of the hydrazine group, we were able to build fused systems with two nitrogen atoms, which allowed us to screen this class of molecules biologically. Thus, Compound **2** was created by reacting the hydrazine-pyrimidine derivative 4-(4-cyanophenyl)-2-hydrazineyl-6-oxo-1,4,5,6-tetrahydropyrimidine-5-carbonitrile with an excess of ethyl acetoacetate **Scheme (3)**. The two C=O groups and the NH group had absorption bands at v=3250 cm^{-1} and 1735, 1687 cm^{-1}, respectively, in Compound **3** infrared spectra. On the other hand, the pyranone proton was detected at δ = 5.8 ppm in the ^{1}H-NMR spectrum, along with two CH_3 protons at δ = 2.46 and 2.49 ppm and an NH proton at δ = 8.05 ppm. The process of treating compound 4-(4-cyanophenyl)-2-hydrazineyl-6-oxo-1,4,5,6-tetrahydropyrimidine-5-carbonitrile with p-nitrobenzaldehyde yielded the Schiff base(E)-4-(4-cyanophenyl)-2-(2-(4-nitrobenzylidene)hydrazineyl)-6-oxo-1,4,5,6-tetrahydropyrimidine-5-carbonitrile **Scheme (3)**. The ^{1}H-NMR spectra showed a singlet for the azomethine proton (N=CH) at δ 8.4 and a broad peak for NH (D_2O exchangeable) at δ 10.8.

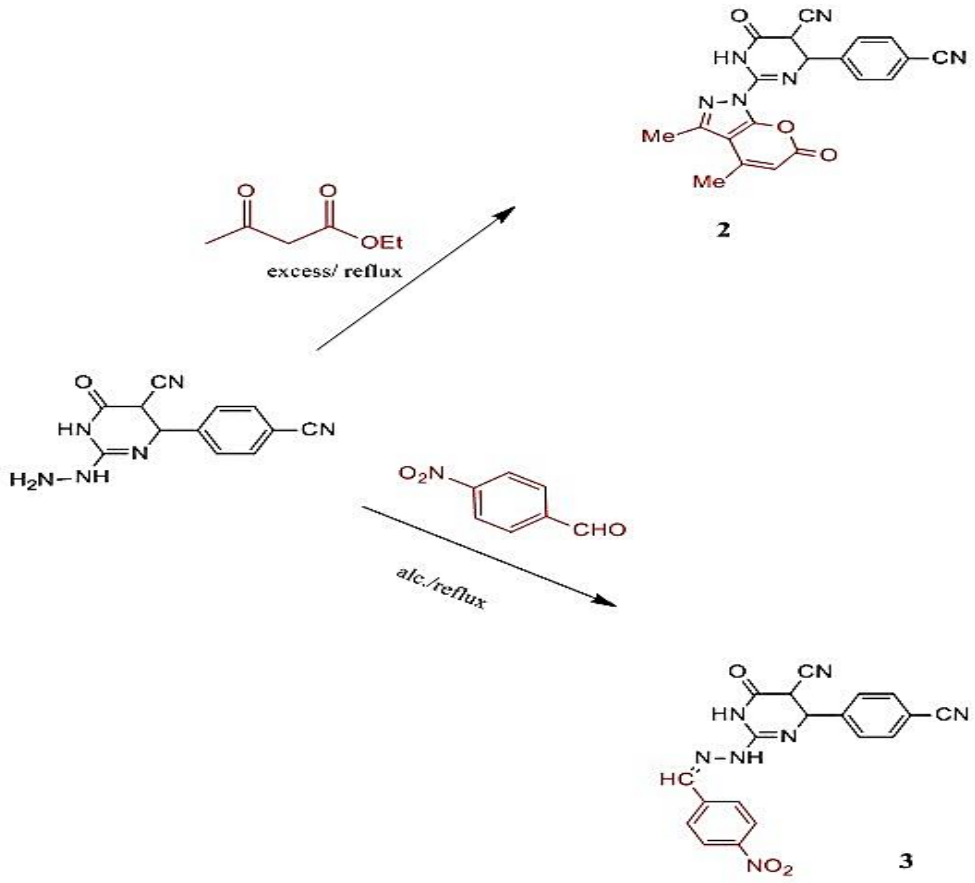

Scheme 3 : Synthsis pyrimidinone derivatives

Computational Chemistry

Molecular docking study:

A molecular docking analysis was conducted using MOE (ver.2022) to confirm the interaction between synthetic compounds and targets associated with anti-cancer illness. All 3 targets associated with anti-cancer illness were docked separately with each medication. These compounds have extraordinarily high binding affinities for all 3 anticancer targets.

all the compounds interacted with the maximum number of targets. Compound **1** demonstrated the most interactions, interacting with four anti-cancer associated targets (5V67, 3FC2, 3IG7, 4ASD) **Table (1)**.

BRD4 has two binding sites: acetyllysine (KAC) and ATP (Jung et al., 2014). Volasertib (BI 6727) is a powerful anticancer drug that inhibits BRD4. Volasertib binds in a pocket between the KAC and ATP binding sites, interacting with Asp144. Volasertib's benzamide moiety contributes to increased hydrophobic exposure (Karim et al., 2021). **Figure (2)** depicts volasertib's binding location to BRD4 (PDB ID:5V67) in 2D and 3D.

Compounds **1**, **2** and **3** bind to BRD4's active site similarly to the native ligand. Compound **1** established a pi-H with ILE 146, a crucial amino acid. Compounds **2** and **3** lacked the H-bond interaction with GLN85 and TYR97, respectively. shown in **Figure (3)**.

Table 1. The binding scores & RMSD values of the promising compounds for Anti-cancer with different enzymes

PDB ID								
	5V67		3FC2		3I G7		4ASD	
	Score (Kcal/mol)	RMSD	Score (Kcal/mol)	RMSD	Score (Kcal/mol)	RMSD	Score (Kcal/mol)	RMSD
1	-7.33488655	1.63391125	-7.17084789	1.69363332	--7.79987192	1.19662356	-7.22580099	1.4002285
2	-6.82293797	1.28724766	-6.28043079	1.07900465	-6.7549367	1.86359692	-7.39949751	1.80180752
3	-7.37499475	1.4097811	-7.02205229	1.27376676	-7.57616806	2.08884525	-6.96619749	1.80570555

Table 2. Docking scores and amino acids involved in interactions for compounds **1**, **2**, and **3** with the binding site of BRD4 (PDB ID: 5V67) compared to the reference ligand volasertib.

Compounds	*Docking score (Kcal/mol)*	*Amino acid H-bond (Bond length Å)*
1	-7.33488655	ILE 146 (A) (4.11)
2	-6.82293797	GLN 85 (A) (3.17)
3	-7.37499475	TYR 97 (A) (3.15)
Volasertib	-7.5325923	ASP 144 (A) (3.60, 3.20)

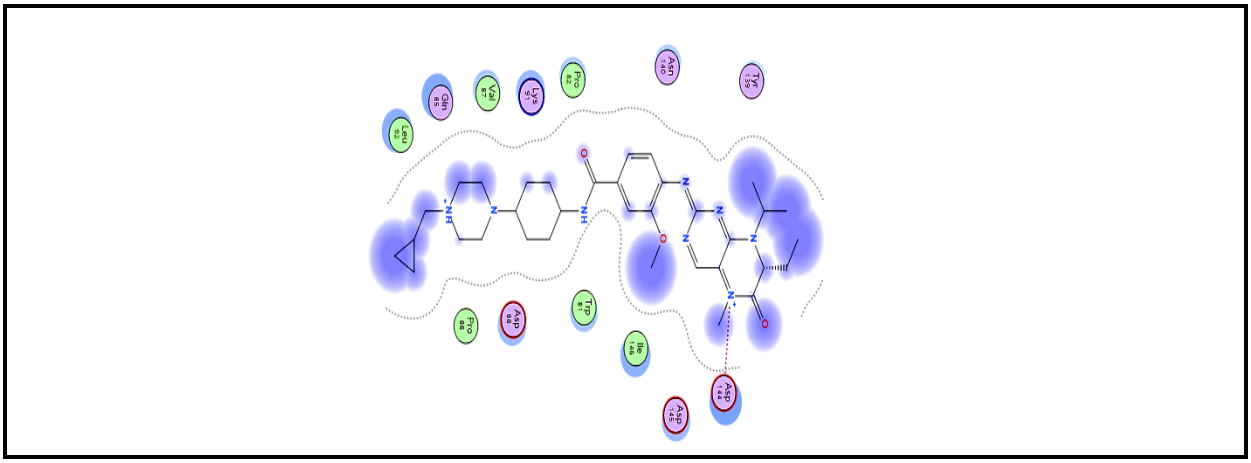

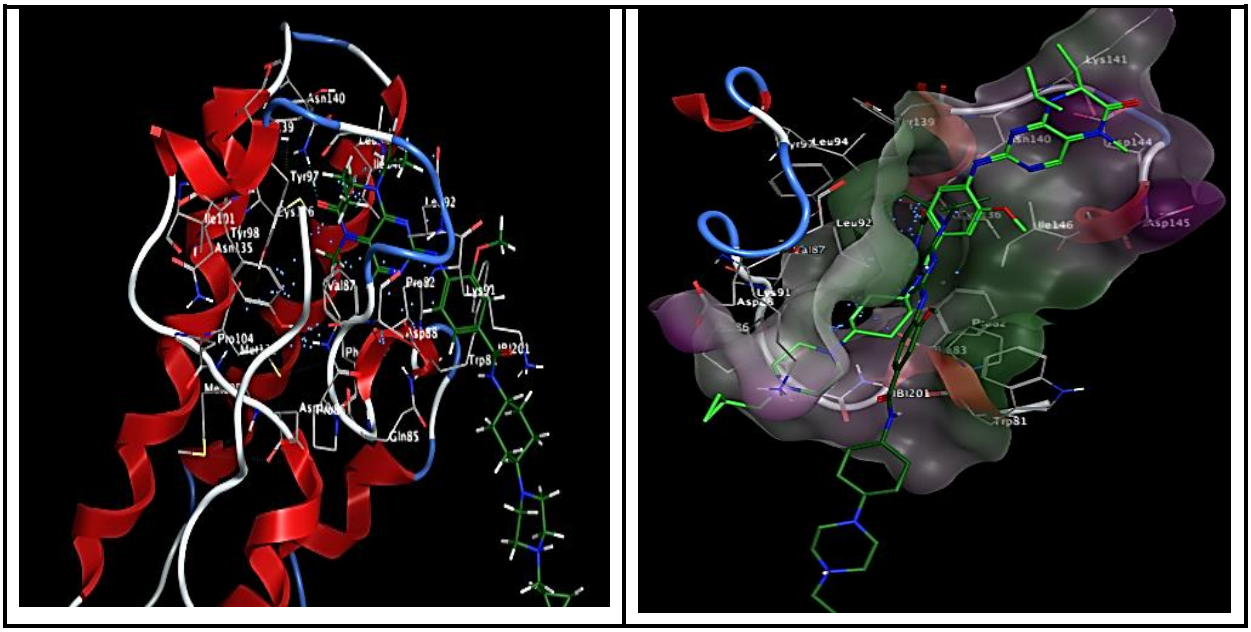

Figure 2. Two- and three-dimensional representations of volasertib (green) at the binding site of BRD4 (PDB ID:5V67)

Comp.	Two- dimensional representations	Three- dimensional representations
1	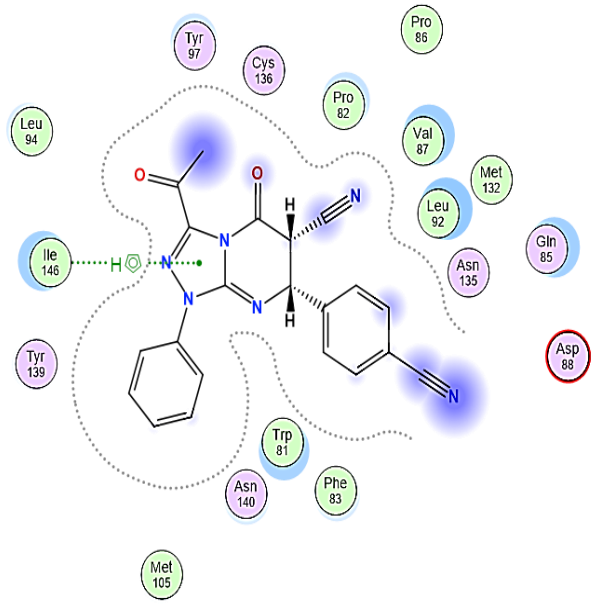	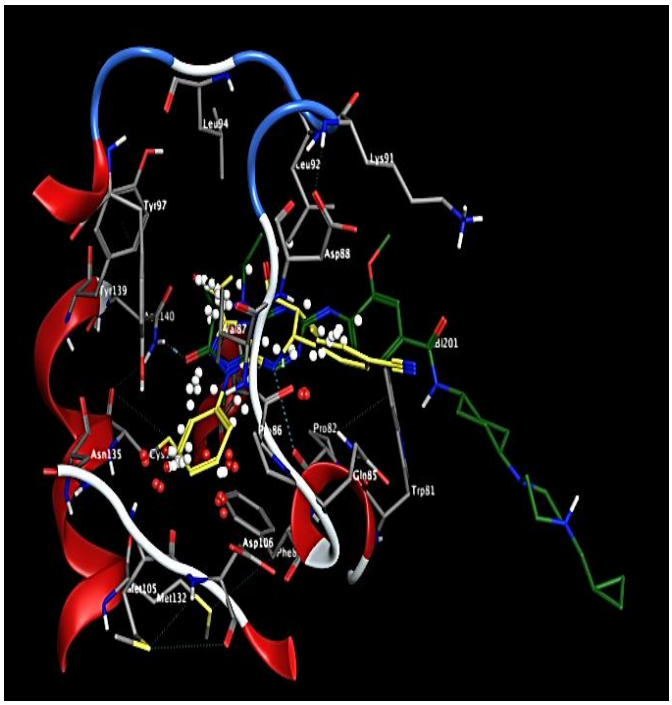

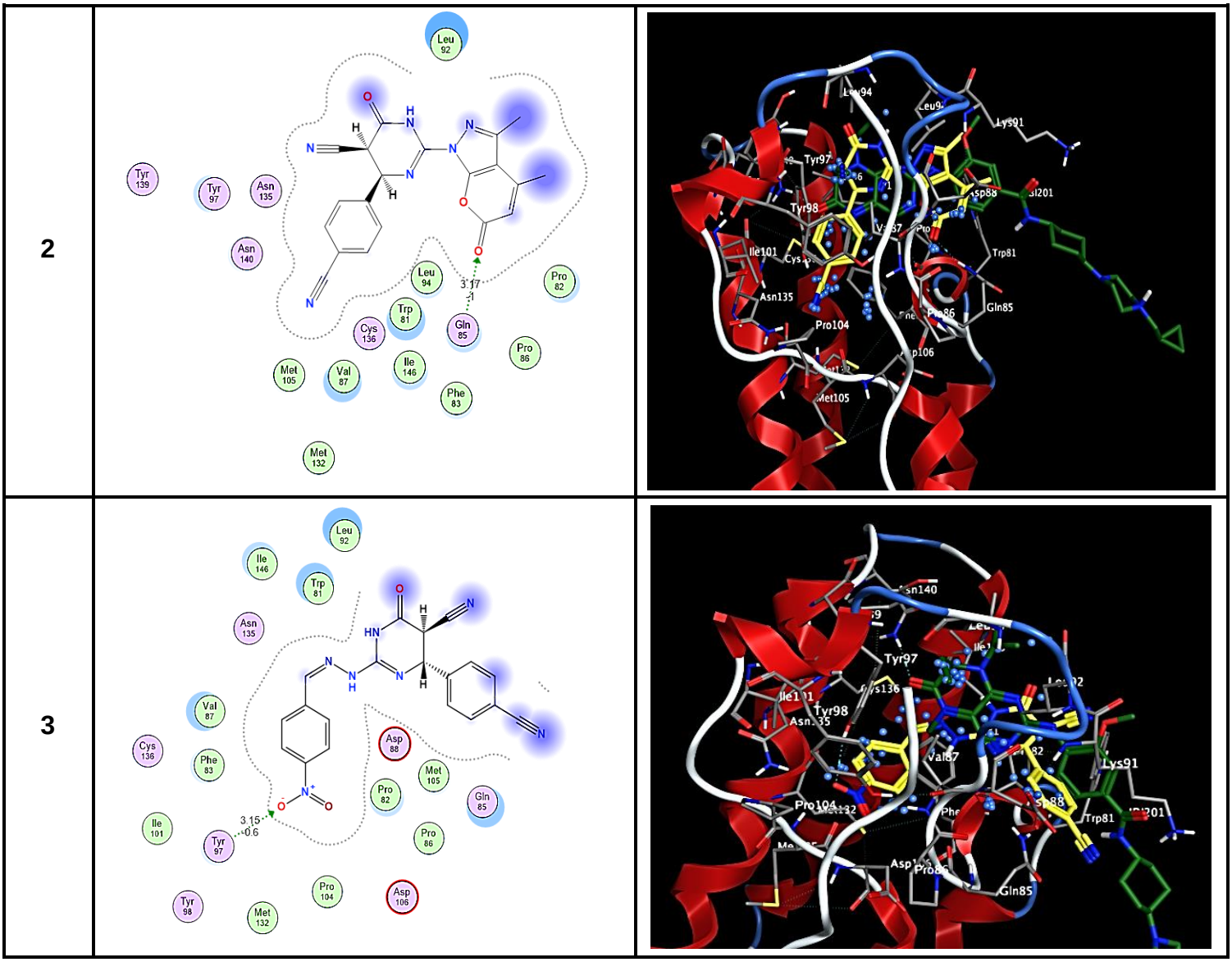

Figure 3. Two-dimensional representations and alignment of compounds **1**, **2** and **3** (Yellow) with volasertib (green) at the binding site of BRD4 (PDB ID:5V67)

The Predicted Drug-Likeness and ADME Properties

The most exciting chemicals, **1**, **2**, and **3**, were put to the anticipated bioinformatics analysis to predict their physicochemical and pharmacokinetic properties, as well as if they may be oral bioavailable medication candidates in contrast to volasertib. The Swiss ADME online tool was used to investigate compounds' drug-likeness and ADME characteristics. The test compounds had good oral bioavailability and excellent physicochemical characteristics, including size (MW between 150 and 500 g/mol), lipophilicity (Log P between -0.7 and +5.0), solubility (Log S less than 6), polarity (TPSA between 20 and 140 Å), and flexibility (maximum 10 rotatable bonds). Compounds were found to vary from being moderately soluble to soluble, in contrast to the reference volasertib, which is poorly soluble utilizing **(Ali, Camilleri, Brown, Hutt, & Kirton, 2012; Daina et al., 2017)**. Furthermore, all tested compounds obeyed Lipinski's rule of five **(Lipinski, Lombardo, Dominy, & Feeney, 2012)**, which includes M.wt. ≤ 500 g/mol, log P ≤ 5, TPSA ≤ 140 Å, HBA ≤ 10, and HBD < 5 **(Ertl, Rohde, & Selzer, 2000)**. This outperforms the reference medicine, volasertib, as seen in **Table (3)**. The molecular weights of the compounds varied from 382.37 to 387.35 g/mol, with volasertib exceeding the optimal range (618.81 g/mol). All orally accessible medication candidates demonstrated an acceptable water/octanol partition coefficient (iLog P) of <5 **(Daina, Michielin, & Zoete, 2014)**. Compounds revealed optimal TPSA values ranging from 116.83 to 159.26 Å. In terms of the number of H-bond acceptor (6-7) and donor (0-2) groups, all compounds followed Lipinski's rule. Furthermore, compounds exhibited an appropriate amount of

rotatable bonds ranging from 3 to 5, as opposed to volasertib, which had 11 rotatable bonds. **Table (3)** shows the physicochemical characteristics and drug-likeness of compounds **1**, **2**, and **3**, as compared to volasertib.

Furthermore, the ADME characteristics investigation revealed that substances might be absorbed through the gut wall, with the white of the egg model **(Daina & Zoete, 2016)** showing significant GI absorption for all compounds. The study discovered that the chemicals could not be passively transported over the blood-brain barrier, as demonstrated by the egg yolk model **[17]**, suggesting that there were no adverse effects on the CNS. Finally, except for compound **3**, none of the drugs inhibited the liver metabolizing enzyme Cytochrome P450 (CYP2D6), indicating no liver adverse effects. **Table (4)** compares the ADME study results for compounds **1**, **2**, and **3** to those of volasertib. Overall, all of the rule principles that might indicate drug-likeness for the examined compounds **1**, **2**, and **3** had outstanding values, suggesting that these substances may meet the cell membrane permeability and bioavailability criteria.

Table 3. The predicted physicochemical characteristics and drug-likeness for compounds **1**, **2**, and **3**, compared to volasertib

Compounds	[a] M.W. (g/mol)	[b] iLog $P_{o/w}$	[c] Log S	[d] TPSA (Å)	[e] HBA	[f] HBD	[g] NRB	Lipinski Violations
1	382.37	1.81	-3.87*	116.83	6	0	3	0
2	386.36	1.61	-3.86*	137.07	7	1	2	0
3	387.35	1.04	-4.59**	159.29	7	2	5	0
Volasertib	618.81	3.50	-6.55***	106.17	7	2	11	2

[a] MW, molecular weight; [b] Log *Po*/w, partition coefficient octanol/water; [c] Log S, Aqueous solubility (* soluble, ** moderately soluble, *** poorly soluble); [d] TPSA, topological polar surface area; [e] HBA, number of H-bond acceptors; [f] HBD, number of H-bond donors; [g] NRB, number of rotatable bonds

Table 4. The predicted ADME study results for compounds 4, 12 and 16 compared to volasertib

Compounds	BBB Permeant	GI Absorption	Cytochrome P450 (CYP2D6 Inhibitor)
4	NO	High	NO
12	NO	High	NO
16	NO	Low	NO
Volasertib	NO	High	NO

VI. CONCLUSION

This study emphasizes the role of molecular docking in cancer drug discovery by examining the interactions between synthetic compounds and cancer-related targets. Using MOE (Molecular Operating Environment, version 2022), the docking analysis evaluated the binding affinities of three synthetic compounds (Compounds 1, 2, and 3) with three anticancer targets.

All compounds exhibited strong binding affinities with the three targets, Compounds 1, 2, and 3 showed interactions with the BRD4 active site similar to those of Volasertib, a known anticancer drug, Additionally, these compounds demonstrated better drug-likeness and pharmacokinetic properties compared to Volasertib, indicating their potential to be more effective and better tolerated.

This research highlights the potential of these new compounds in the development of enhanced cancer therapies.

ACKNOWLEDGMENT

The authors are very thankful to Zagazig University, Science faculty and Chemistry department for Supporting Project to complete.

CONFLICT OF INTEREST

The authors declare that they have no conflicts of interest.

V. REFERENCE

Ali, J., Camilleri, P., Brown, M. B., Hutt, A. J., & Kirton, S. B. (2012). In silico prediction of aqueous solubility using simple QSPR models: the importance of phenol and phenol-like moieties. *Journal of chemical information and modeling*, *52*(11), 2950-2957.

Aziz, M. A., Shehab, W. S., Al-Karmalawy, A. A., EL-Farargy, A. F., & Abdellattif, M. H. (2021). Design, Synthesis, Biological Evaluation, 2D-QSAR Modeling, and Molecular Docking Studies of Novel 1H-3-Indolyl Derivatives as Significant Antioxidants. *International Journal of Molecular Sciences, 22*(19), 10396.

Bray, F., Ferlay, J., Soerjomataram, I., Siegel, R. L., Torre, L. A., & Jemal, A. (2018). Global cancer statistics 2018: GLOBOCAN estimates of incidence and mortality worldwide for 36 cancers in 185 countries. *CA: a cancer journal for clinicians, 68*(6), 394-424.

Daina, A., Michielin, O., & Zoete, V. (2014). iLOGP: a simple, robust, and efficient description of n-octanol/water partition coefficient for drug design using the GB/SA approach. *Journal of chemical information and modeling, 54*(12), 3284-3301.

Daina, A., Michielin, O., & Zoete, V. (2017). SwissADME: a free web tool to evaluate pharmacokinetics, drug-likeness and medicinal chemistry friendliness of small molecules. *Scientific reports, 7*(1), 42717.

Daina, A., & Zoete, V. (2016). A boiled-egg to predict gastrointestinal absorption and brain penetration of small molecules. *ChemMedChem, 11*(11), 1117-1121.

Dong, R., Zhang, C., Wang, C., Zhou, X., Li, W., Zhang, J.-Y., . . . Sun, L.-P. (2022). Design, synthesis and anticancer evaluation of 3-methyl-1H-indazole derivatives as novel selective bromodomain-containing protein 4 inhibitors. *Bioorganic & Medicinal Chemistry, 55*, 116592.

El-Kalyoubi, S., El-Sebaey, S. A., Elfeky, S. M., Al-Ghulikah, H. A., & El-Zoghbi, M. S. (2023). Novel Aminopyrimidine-2, 4-diones, 2-Thiopyrimidine-4-ones, and 6-Arylpteridines as Dual-Target Inhibitors of BRD4/PLK1: Design, Synthesis, Cytotoxicity, and Computational Studies. *Pharmaceuticals, 16*(9), 1303.

Elfeky, S. M., Almehmadi, S. J., & Tawfik, S. S. (2022). Synthesis, in-silico, and in-vitro study of novel chloro methylquinazolinones as PI3K-δ inhibitors, cytotoxic agents. *Arabian Journal of Chemistry, 15*(2), 103614.

Elkady, H., El-Adl, K., Sakr, H., Abdelraheem, A. S., Eissa, S. I., & El-Zahabi, M. A. (2023). Novel promising benzoxazole/benzothiazole-derived immunomodulatory agents: Design, synthesis, anticancer evaluation, and in silico ADMET analysis. *Archiv der Pharmazie, 356*(9), 2300097.

Ertl, P., Rohde, B., & Selzer, P. (2000). Fast calculation of molecular polar surface area as a sum of fragment-based contributions and its application to the prediction of drug transport properties. *Journal of medicinal chemistry, 43*(20), 3714-3717.

Faivre, E. J., McDaniel, K. F., Albert, D. H., Mantena, S. R., Plotnik, J. P., Wilcox, D., . . . Wang, L. (2020). Selective inhibition of the BD2 bromodomain of BET proteins in prostate cancer. *Nature, 578*(7794), 306-310.

Hamed, E. O., Assy, M. G., Ouf, N. H., Elsayed, D. A., & Abdellattif, M. H. (2022). Cyclization of N-acetyl derivative: Novel synthesis–azoles and azines, antimicrobial activities, and computational studies. *Heterocyclic Communications, 28*(1), 35-43.

Hamed, E. O., Elsayed, D. A., Assy, M. G., & Shehab, W. S. (2022). Design, Synthesis, Docking, 2D-QSAR Modelling, Anticancer and Antioxidant Evaluation of Some New Azo-Compounds Derivatives and Investigation of Their Fluorescence Properties. *ChemistrySelect, 7*(41), e202202534.

Jung, M., Philpott, M., Müller, S., Schulze, J., Badock, V., Eberspächer, U., . . . Fernández-Montalván, A. (2014). Affinity map of bromodomain protein 4 (BRD4) interactions with the histone H4 tail and the small molecule inhibitor JQ1. *Journal of biological chemistry, 289*(13), 9304-9319.

Karim, R. M., Bikowitz, M. J., Chan, A., Zhu, J.-Y., Grassie, D., Becker, A., . . . Schonbrunn, E. (2021). Differential BET bromodomain inhibition by dihydropteridinone and pyrimidodiazepinone kinase inhibitors. *Journal of medicinal chemistry, 64*(21), 15772-15786.

Kukol, A. (2008). *Molecular modeling of proteins* (Vol. 443): Springer.

Kumar, R., Kumar, V., Kamal, R., Kumar, A., Kaur, S., Bansal, A., & Chetti, P. (2022). 2, 4-Bis (2-(E)-arylidenehydrazinyl) quinazolines: Expeditious Synthesis, Characterization, Antiproliferative Effects against Breast Cancer Cell Line and Molecular Docking Studies. *ChemistrySelect, 7*(38), e202202635.

Lambert, J.-P., Picaud, S., Fujisawa, T., Hou, H., Savitsky, P., Uusküla-Reimand, L., . . . Tucholska, M. (2019). Interactome rewiring following pharmacological targeting of BET bromodomains. *Molecular cell, 73*(3), 621-638. e617.

Lipinski, C. A., Lombardo, F., Dominy, B. W., & Feeney, P. J. (2012). Experimental and computational approaches to estimate solubility and permeability in drug discovery and development settings. *Advanced drug delivery reviews, 64*, 4-17.

Mabrouk, R. R., Abdallah, A. E., Mahdy, H. A., El-Kalyoubi, S. A., Kamal, O. J., Abdelghany, T. M., . . . El-Zahabi, M. A. (2023). Design, synthesis, and biological evaluation of new potential unusual modified anticancer immunomodulators for possible non-teratogenic quinazoline-based thalidomide analogs. *International Journal of Molecular Sciences, 24*(15), 12416.

Mao, F., Li, J., Luo, Q., Wang, R., Kong, Y., Carlock, C., . . . Liu, X. (2018). Plk1 inhibition enhances the efficacy of BET epigenetic reader blockade in castration-resistant prostate cancer. *Molecular cancer therapeutics, 17*(7), 1554-1565.

Mokhtari, R. B., Homayouni, T. S., Baluch, N., Morgatskaya, E., Kumar, S., Das, B., & Yeger, H. (2017). Combination therapy in combating cancer. *Oncotarget, 8*(23), 38022.

Morris, G. M., & Lim-Wilby, M. (2008). Molecular docking *Molecular modeling of proteins* (pp. 365-382): Springer.

Penna, L. S., Henriques, J. A. P., & Bonatto, D. (2017). Anti-mitotic agents: Are they emerging molecules for cancer treatment? *Pharmacology & therapeutics, 173*, 67-82.

Picaud, S., Wells, C., Felletar, I., Brotherton, D., Martin, S., Savitsky, P., . . . Lingard, H. (2013). RVX-208, an inhibitor of BET transcriptional regulators with selectivity for the second bromodomain. *Proceedings of the National Academy of Sciences, 110*(49), 19754-19759.

Rudolph, D., Steegmaier, M., Hoffmann, M., Grauert, M., Baum, A., Quant, J., . . . Adolf, G. n. R. (2009). BI 6727, a Polo-like kinase inhibitor with improved pharmacokinetic profile and broad antitumor activity. *Clinical cancer research, 15*(9), 3094-3102.

Saleh, A. M., Mahdy, H. A., El-Zahabi, M. A., Mehany, A. B., Khalifa, M. M., & Eissa, I. H. (2023). Design, synthesis, in silico studies, and biological evaluation of novel pyrimidine-5-carbonitrile derivatives as potential anti-proliferative agents, VEGFR-2 inhibitors and apoptotic inducers. *RSC advances, 13*(32), 22122-22147.

Seal, J., Lamotte, Y., Donche, F., Bouillot, A., Mirguet, O., Gellibert, F., . . . Beinke, S. (2012). Identification of a novel series of BET family bromodomain inhibitors: binding mode and profile of I-BET151 (GSK1210151A). *Bioorganic & medicinal chemistry letters, 22*(8), 2968-2972.

Shehab, W. S., Amer, M. M., Elsayed, D. A., Yadav, K. K., & Abdellattif, M. H. (2023). Current progress toward synthetic routes and medicinal significance of quinoline. *Medicinal Chemistry Research, 32*(12), 2443-2457.

Shehab, W. S., Elsayed, D. A., Abdel Hamid, A. M., Assy, M. G., Mouneir, S. M., Hamed, E. O., . . . El-Bassyouni, G. T. (2024). CuO nanoparticles for green synthesis of significant anti-Helicobacter pylori compounds with in silico studies. *Scientific reports, 14*(1), 1608.

Umar, A., Faidallah, H. M., Ahmed, Q. U., Alamry, K. A., Mukhtar, S., Alsharif, M. A., . . . Hussien, M. A. (2022). Design, synthesis, in vitro antiproliferative effect and in situ molecular docking studies of a series of new benzoquinoline derivatives. *Journal of King Saud University-Science, 34*(4), 102003.

Vann, K. R., Pal, D., Morales, G. A., Burgoyne, A. M., Durden, D. L., & Kutateladze, T. G. (2020). Design of thienopyranone-based BET inhibitors that bind multiple synthetic lethality targets. *Scientific reports, 10*(1), 12027.

Watts, E., Heidenreich, D., Tucker, E., Raab, M., Strebhardt, K., Chesler, L., . . . Hoelder, S. (2019). Designing dual inhibitors of anaplastic lymphoma kinase (ALK) and bromodomain-4 (BRD4) by tuning kinase selectivity. *Journal of medicinal chemistry, 62*(5), 2618-2637.

Wyce, A., Ganji, G., Smitheman, K. N., Chung, C.-w., Korenchuk, S., Bai, Y., . . . McCabe, M. T. (2013). BET inhibition silences expression of MYCN and BCL2 and induces cytotoxicity in neuroblastoma tumor models. *PloS one, 8*(8), e72967.

Yuzwa, S. A., Borrett, M. J., Innes, B. T., Voronova, A., Ketela, T., Kaplan, D. R., . . . Miller, F. D. (2017). Developmental emergence of adult neural stem cells as revealed by single-cell transcriptional profiling. *Cell reports, 21*(13), 3970-3986.

Zhang, J., Yang, P. L., & Gray, N. S. (2009). Targeting cancer with small molecule kinase inhibitors. *Nature reviews cancer, 9*(1), 28-39.